





Research Article

Crosslinking, Mechanical Properties, and Antimicrobial Activity of Photocurable Diacrylate Urethane/ZnO-Ag Nanocomposite Coating

Truc Vy Do ^{1,2} Minh Nguyet Ha ^{1,2} Tuan Anh Nguyen ¹ Hoang Thu Ha ³
and Thien Vuong Nguyen ^{1,2}

¹Institute for Tropical Technology, VAST, 18 Hoang Quoc Viet, Cau Giay, Hanoi, Vietnam

²Graduate University of Science and Technology, VAST, 18 Hoang Quoc Viet, Cau Giay, Hanoi, Vietnam

³University of Education-Vietnam National University, 144 Xuan Thuy, Cau Giay, Hanoi, Vietnam

Correspondence should be addressed to Hoang Thu Ha; hoangthuhavnuued@gmail.com
and Thien Vuong Nguyen; vuongvast@gmail.com

Received 22 June 2021; Revised 4 August 2021; Accepted 26 October 2021; Published 9 November 2021

Academic Editor: George Kyzas

Copyright © 2021 Truc Vy Do et al. This is an open access article distributed under the Creative Commons Attribution License, which permits unrestricted use, distribution, and reproduction in any medium, provided the original work is properly cited.

In this article, ZnO-Ag nanohybrids were chemically synthesized in the aqueous medium by reducing silver nitrate with sodium borohydride NaBH₄. These nanohybrids were then homogeneously dispersed into the diacrylate urethane/1,6-hexanediol diacrylate resin system at a content of 2 wt%. The structural morphology, mechanical resistances, and crosslinking of the as-prepared nanocomposite coating (nanocoating) were evaluated. The antimicrobial characteristic was tested by keeping track of the lag-log growth phase of *E. coli* bacteria in the coating existence among cell cultures. The obtained data indicated that the nanohybrids added into the UV curing diacrylate urethane matrices had significantly increased the abrasion resistance, relative hardness, and conversion of the acrylate groups of the nanocoating. In addition, the antibacterial test revealed that the nanocoating had good antibacterial property against *E. coli*, whereas for the pure coating (without ZnO-Ag nanoparticles), there was no antibacterial activity observed.

1. Introduction

UV curable acrylate resin-based paints exhibit many advantages, such as transparency, moisture resistance, chemical resistance, and being environmentally friendly, since they do not contain the organic solvents and can be processed at normal temperatures. Consequently, they have been widely applied to various finish surfaces, such as steel or wooden floors [1–4].

Nowadays, nanomaterials attract strong research and application interest. The addition of nanoscale additives to the polymer matrix significantly enhanced the properties of the material [5–12]. Enhancing the properties of coatings with antibacterial function has become a social demand; thus, there is an attempt to mix inorganic nanoparticles (like Ag, ZnO, and TiO₂) as antibiotics into paint [13–19]. Among those, Ag nanoparticles showed the highest anti-

microbial effectiveness against most bacteria. In order to improve the antimicrobial activity of nano-Ag, Ag particles are often attached to nanosized transition metal oxides (such as Fe₃O₄ and MnO₂ nanoparticles). In the previously published paper, we reported the antimicrobial activity of Fe₃O₄-Ag hybrid nanoparticles which was clearly more efficient than that of the single Ag nanoparticles [20–23]. The plausible explanation for this observation is that (1) Ag⁺ ions were released faster from the hybrid nanoparticles and (2) the ionization of nano-Ag was accelerated by the presence of Fe³⁺ ions. Moreover, the absorbed radiation range of the nanohybrids can shift to the UV and visible light region [20].

However, the addition of nanoparticles (as nanofillers) can affect the curing reaction of thermoset resin systems depending on the intrinsic composition of the nanoparticles. In case of the epoxy matrix, Fe₃O₄ nanoparticles can act as a

bridging link molecule, leading to reduce the total free mass and increase the cross-linking density [24, 25]. Herein, to explore the healing dynamics of the epoxy/amine system, Fe₃O₄ nanoparticles played a role as nanocontainers for carrying functional groups such as the carboxylic acid [26], amino [27, 28], or hydroxyl [27, 29]. The authors found that reaction between carboxylic acid and amine functional groups of curing agent could impact hardener activation [26]. In contrast, hydroxyl and amine groups could increase the amount of thermal curing by gaining access to the epoxy groups [27]. It was reported that nano-SiO₂ might cause an incomplete crosslinking stage of clearcoat based on acrylic-melamine resin, reducing the crosslinking density of the neat clearcoat, and enhancing the weathering durability of the clearcoats. One possible explanation is that nano-SiO₂ absorbed the UV light, thus protecting the clearcoat from the impact of weathering degradation [30]. In our previous works [31–33] when examining the curing reaction of acrylic polyols with isocyanate, we found that isocyanate groups are also involved in reaction with OH groups of nano-SiO₂ to form a tight inorganic-organic hybrid material. For UV curing systems, the degree of influence of additives depends not only on the content but also on their ability to absorb UV rays and photocatalytic activity. Fe₃O₄-Ag hybrid nanoparticles, despite a strong UV absorption, their low content (0.1 wt%) might not significantly affect the kinetics of curing reaction [23]. The organic UV absorber T384 reduced the efficiency of double bonds while nanoparticles absorb UV anatase TiO₂ and ZnO increased the conversion of the acrylate groups of the system due to strong photocatalytic activity [34].

In this work, ZnO-Ag nanohybrids were chemically synthesized in the aqueous medium by reducing silver nitrate with sodium borohydride NaBH₄. Their structural morphology had been characterized. These nanohybrids were then homogeneously dispersed into the diacrylate urethane/1,6-hexanediol diacrylate resin system. The photocrosslinking polymerization process of the system of acrylate urethane resin and 1,6 hexanediol diacrylate diluent in the presence of ZnO-Ag nanohybrids had been investigated by using various measurements, such as the quantitative infrared spectra, coating hardness, and coating gel fraction. In addition, morphology, abrasion resistance, and antimicrobial activity of nanocomposite coating were also evaluated.

2. Experiments

2.1. Chemicals. NaBH₄, AgNO₃, and nano-ZnO were ordered from Sigma-Aldrich.

A photocurable resin system includes (i) Ebecryl 284 diacrylate urethane resin (abbrev. E284) ordered from a Radcure Specialties, (ii) 1,6-hexanediol diacrylate diluent (abbrev. HDDA, 80%, Sigma), and (iii) 1-hydroxy-cyclohexyl-phenyl-ketone photoinitiator, Irgacure 184 (I-184, CIBA). Figure 1 represents chemical structure of components of the photocurable resin system.

2.2. Synthesis of ZnO-Ag Nanohybrids. ZnO-Ag nanohybrids are chemically synthesized in the aqueous medium by reduc-

ing silver nitrate with sodium borohydride NaBH₄ [11]. Firstly, nano-ZnO (1.5 g) is added in 300 ml of distilled water, then dispersed homogeneously with aid of the ultrasonication 35 kHz for 60 min. Next, 30 ml of AgNO₃ solution (1.67 mg/ml) is dripped into the above-prepared dispersion of ZnO nanoparticles by further sonication for 40 min. The mixture is then placed into the 500 ml glass flask for the next synthesis step. To fabricate ZnO-Ag nanohybrids, NaBH₄ solution formed by dissolving 0.024 g of reductant into 50 ml water is then dripped (1 drop/s) to the reaction flask. The mixed solution is stirred (120 rpm for 60 min) at 4°C. The nanoparticles were obtained by repeatedly adding fresh distilled water and then centrifuging the solution at 10,000 rpm for 5 min for several times until the total removal of the residual precursors and agents.

2.3. Preparation of Nanocomposite Coating. ZnO-Ag nanohybrids at the 2 wt% content of HDDA and E284 are added into HDDA, then ultrasonicated during 3 hrs. Thereafter, this mixture is mixed with E284 and I.184 by mechanical stirring in the Ika RW16 Basic Mixer (England) for 30 min. The ratio of HDDA/E284/I.184 was 45/55/3.

The paint films are prepared on different surfaces with varied sizes depending on investigation purposes. In detail, for IR spectral analysis, paint layers with a 25 μm thickness are coated on KBr pellets. For gel fraction examination and morphology observation, the coatings were made on Teflon sheets with the size of 100 × 100 × 10. The coatings were deposited on glass plates (100 × 100 × 3 mm) for testing the abrasion resistance and relative hardness.

The coating samples are exposed to UV light (250 mW/cm²) using the FUSION UV system (F300S, USA) at 25°C in air by passing several times with a 5–40 m/s rate of web. The time of UV exposure can calculate from the web rate, for example, UV exposure time of 0.15 s corresponds to a web pass at 40 m/s.

2.4. Characterizations

2.4.1. FTIR Spectrum Analysis. A decrease of characteristic IR absorption bands of acrylate groups during the crosslinking reaction is quantitatively studied according to the method described in previous papers [23, 34] by using a FTIR spectroscopy Nicolet iS10 (USA).

2.4.2. Gel Fraction Analysis. The gel fraction (GEL) of coatings is analyzed according to ASTM D 2765. The cured samples are carried out in a Soxhlet tool in CH₃COCH₃ for 24 h [23]. The GEL is determined by the following formula:

$$\text{The GEL(\%)} = \left(\frac{m_t}{m_0} \right) \times 100, \quad (1)$$

where m_t is the weight of insoluble part which was heated at 50°C until completely dry and m_0 was the weight of initial coating (before analysis).

2.4.3. Study on Hardness and Abrasion Resistance of Coatings. The hardness of paint film is evaluated based on the NF T 30-016 standard by using a pendulum damping

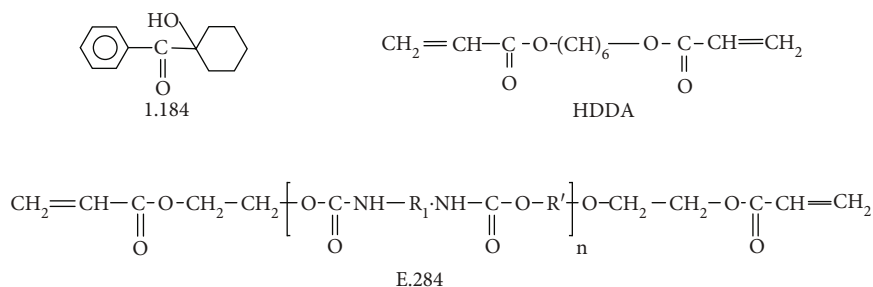


FIGURE 1: Chemical structure of the photocurable resin system.

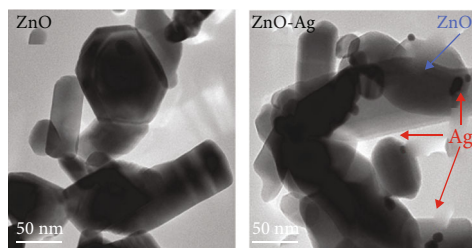


FIGURE 2: TEM images of pure ZnO nanoparticles (ZnO) and self-synthesis ZnO-Ag nanohybrids.

tester (model 300). The relative hardness (RH) is calculated by the formula as follows:

$$RH = \frac{\text{Absolute hardness of the film}}{425 \text{ (425 was absolute hardness of standard glass)}} \quad (2)$$

The abrasion resistance of the films is determined according to the abrasive falling methods (ASTM D968). Each sample was tested 3 times, and the illustrated results were the average values.

2.4.4. Microstructural Examination. The morphology of the self-synthesized ZnO-Ag nanohybrids has been analyzed by transmission electron microscopy (JEM 1010, JEOL Ltd., Tokyo, Japan). The crystallinity and crystalline phase of the fabricated nanoparticle structures were examined using an X-ray diffractometer (XRD, Philips X'Pert MPD) with $\text{CuK}\alpha$ radiation (0.1540 nm) in the range of 20° – 60° .

The morphology of the nanocomposite coating has been studied using Field Emission Scanning Electron Microscopy S 4800 (FE-SEM) (Hitachi, Japan).

2.4.5. Antimicrobial Assay. For antimicrobial assay, *E. coli* strain DH5 α is received from Invitrogen (USA); LB medium including yeast extract and Bacto tryptone are ordered from Merck (Germany). *E. coli* strain DH5 α is inoculated into 2 ml of LB medium and shacked overnight at 200 rpm while the temperature remained 37°C . Another cell suspension at 1% *v/v* cultured cell suspension: LB medium is prepared by inoculating the cells into 100 ml of fresh LB medium. The incubation underwent the same conditions as presented above. Once the value of optical density value ($\lambda = 600 \text{ nm}$, OD_{600}) was 0.3, the coatings are placed into incubation-

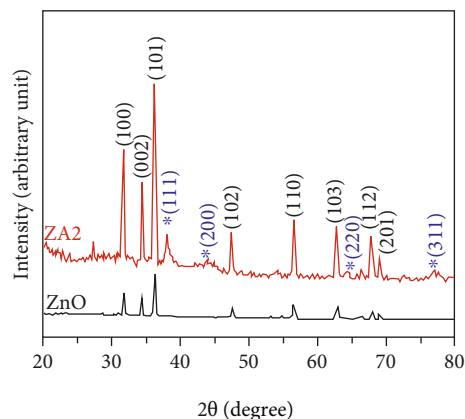


FIGURE 3: XRD diffraction diagrams of pure ZnO nanoparticles (ZnO) and ZnO-Ag nanohybrids (ZA2).

flagon and kept cultivating. The suspension of cultured cell suspension is then collected at various time scales (from 30 to 300 min) after adding either UVAU or UVAU/ZnO-Ag nanocoatings (with the same size of $100 \times 100 \times 0.03 \text{ mm}$); then, their OD_{600} values were determined. All experiments were conducted in triplicate for determining the mean value [19, 23].

3. Results and Discussions

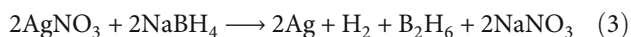
3.1. Study on Characteristics of ZnO-Ag Nanohybrids. The structural morphology of pure ZnO nanoparticles (ZnO) and ZnO-Ag nanohybrids is characterized by TEM and XRD analyses and shown in Figures 2 and 3.

Figure 2 shows that the used commercial ZnO nanoparticles were cylindrical in shape and have dimensions of about 30–70 nm in width and about 100–200 nm in length; Ag nanoparticles are spherical in shape with a size of about 10–30 nm attached to ZnO nanoparticles. Because these two types of particles are different in shape and size, it is easy to see the presence of both types of particles on TEM image.

The crystalline phase structure of the self-synthesized ZnO-Ag nanohybrids is analyzed by the X-ray diffraction method. XRD diffraction diagrams of ZnO-Ag nanohybrids and pure ZnO nanoparticles are presented in Figure 3.

From the obtained results, it can be seen that the XRD diagrams of both particles show characteristic diffraction peaks corresponding to the lattice faces (100), (002), (101), (102), (110), (103), (112), and (201) of ZnO nanoparticles

(JCPDS No. 36-1451). Apart from the spectral lines that characterize the hexagonal crystal structure of pure ZnO compounds, no other peaks or spectra of the impurity were observed. On the XRD diffraction pattern of ZnO-Ag hybrid nanoparticles, the characteristic diffraction peaks of ZnO remain the same, which shows that Ag ions are not substituted for ZnO in the crystal lattice of ZnO. In addition, on the XRD pattern of ZnO-Ag nanohybrid nanoparticles, diffraction peaks appear at angular positions corresponding to the lattice planes (111), (200), (220), and (311) in the face center cubic structure of Ag (JCPDS No. 04-0783). Thus, the method of using NaBH_4 reducing agent to reduce Ag^+ ions to Ag atoms is described by the following reaction equation:



3.2. Study on Crosslinking and Characteristics of Photocuring Acrylate Urethane/ZnO-Ag Nanocoating

3.2.1. Conversion of the Acrylate Groups. Using the IR spectral method to study the crosslinking of the curing resin system is one of the most simple and effective methods. It allows to assess both the rate of polymerization reaction and the conversion of the reacted functional groups [1, 23, 34]. In the current paper, the photocrosslinking polymerization reaction of the coating base on E.284 resin, HDDA diluent, and I.184 photoinitiator in the presence of 2 wt% ZnO-Ag nanohybrids is investigated by analyzing the changes of IR absorption density of acrylate double bonds. IR spectra of the photocurable diacrylate urethane/1,6-hexanediol diacrylate/1-hydroxy-cyclohexyl-phenyl-ketone systems without (UVAU) and with 2 wt% ZnO-Ag nanohybrids (UVAU/ZnO-Ag) before and after UV exposure of 4.8 s are presented in Figure 4.

Figure 4 shows that after 4.8 s exposed to UV, IR bands at 1632, 1409, 984, and 811 cm^{-1} which are assigned to the double bonds of acrylate groups in E.284 and HDDA molecules decreased. Among those, the absorption band at 811 cm^{-1} is chosen to study numerically the transformation of the acrylate groups throughout the crosslinking process of the coatings because of its most clearly decrease. The calculated data are presented in Figure 5.

As shown in Figure 5, the conversion of the acrylate groups occurs rapidly in the first 0.15 s and then slows down. The acrylate double bond conversion at the coating containing 2 wt% ZnO-Ag nanohybrids was higher than that at neat coating (without ZnO-Ag nanohybrids). After 4.8 s exposed to UV light, most of the acrylate double bonds were covered by 93.53 and 95.82% for neat and nanocomposite coatings, respectively. Thus, ZnO-Ag nanoparticles enhanced the transformation of acrylate double bonds.

3.2.2. Variation of Gel Fraction. To have further information of the photopolymerization reaction of the system in the presence of ZnO-Ag nanohybrids, the GEL of the coatings was determined. Figure 6 visualizes the obtained results.

Figure 6 indicates that, after 0.3 s of crosslinking, the GEL of the films without and with 2 wt% the nanohybrids appeared. The GEL increased rapidly in the first 2.4 s; after

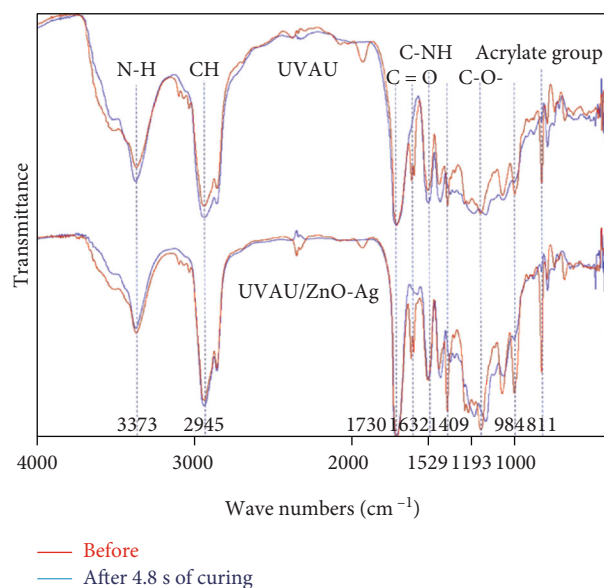


FIGURE 4: IR spectra of the UV-curable E.284/HDDA/I.184 systems without (UVAU) and with 2 wt% ZnO-Ag nanohybrids (UVAU/ZnO-Ag) before and after 4.8 s UV light irradiation.

then, it slowed down. In the presence of 2 wt% of the nanohybrids, the GEL of the film was increased in comparison with that of the neat film. After 4.8 s of the crosslinking, the GEL of the films got the highest value of approximately 95.3 (without the nanohybrids) and 96.7% (with 2 wt% ZnO-Ag nanohybrids). Thus, 2 wt ZnO-Ag nanohybrids increased the GEL of the films.

3.2.3. Hardness Evaluation. For the thermoset resin system, the hardness of the coating increased with the crosslinking density, and thus, it is possible to study the polymerization reaction by keeping track of the growth of the coatings' hardness. Figure 7 represents the relative hardness of coatings varied over time range of 0-4.8 s. It is clear that the hardness values rose rapidly in the first 1.2 s of the reaction before slowing down. The hardness of the coating containing 2 wt% ZnO-Ag nanohybrids was higher than that of the neat coating (without the nanohybrids). After 4.8 s of crosslinking reaction, the hardness of the coating and ZnO-Ag hybrid-reinforced coating reached the highest value of around 0.72 and 0.76, respectively. The incorporation of the nanoparticles in the coating matrix increased slightly the coating hardness.

It is well known that the outstanding characteristic of a photoinitiator is susceptible to UV light [2, 27]. When being exposed to UV light in FUSION UV equipment, the I 184 photoinitiator is destructed into free radicals which then attack the acrylate group, initiating the crosslinking polymerization. At first (in the first 0.15 s of UV exposure), the content of photoinitiators is high (about 3%) and the curing system is relatively flexible (low viscosity) so the reaction of the acrylate double bonds is inconsiderably impacted by UV absorbers of ZnO-Ag nanohybrids. However, concentration of the photoinitiators and the acrylate groups reduce rapidly by time, and thus, the conversion of the acrylate groups

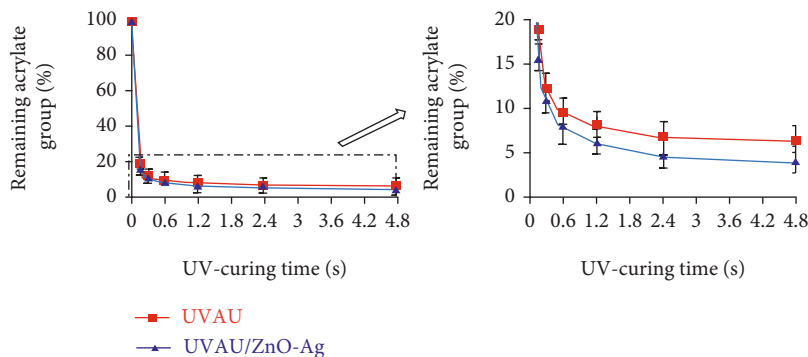


FIGURE 5: Conversion of the acrylate groups under the UV light irradiation.

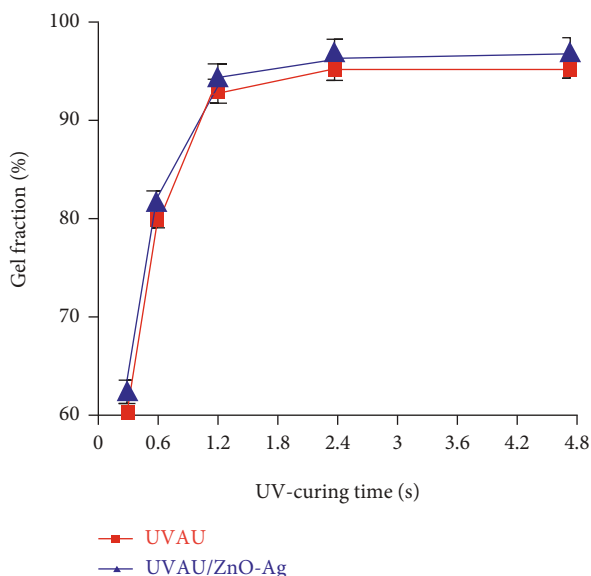


FIGURE 6: Variations of GEL of the photocurable acrylate urethane coating without (UVAU) and with 2 wt% ZnO-Ag nanohybrids (UVAU/ZnO-Ag).

slowed down. In the presence of 2 wt% ZnO-Ag nanohybrids, the conversion of the acrylate groups is affected by photocatalytic characteristic of nano ZnO-Ag hybrid structure. This effect is similar to the case of photocatalyst nanoparticles (A-TiO₂, ZnO) [34–37]. The difference is that due to the hybridization with Ag, the photocatalytic activity of ZnO is reinforced. When absorbing UV energy, an electron jumps from the valence band to the conduction band, resulting in the formation of an electron-hole pair. These electron and positive hole pairs reacted with hydroxyl functional groups, water and oxygen molecules attached to the nanoparticles' surface, generating free radicals (·OH) [38–40] which could also initiate the crosslinking polymerization reaction of acrylate double bonds, leading to the increase of its conversion as well as the increase in the GEL and relative hardness of the film.

3.2.4. Study on Abrasion Resistance of the Paint Film. Abrasion resistance of the films without (UVAU) and with 2 wt% ZnO-Ag nanohybrids (UVAU/ZnO-Ag) after 4.8 s of crosslinking is presented in Figure 8.

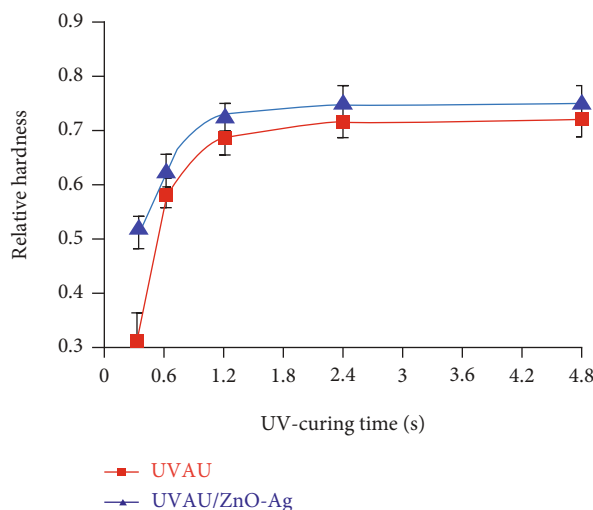


FIGURE 7: Variation of hardness of the films without (UVAU) and with 2 wt% ZnO-Ag nanohybrids (UVAU/ZnO-Ag).

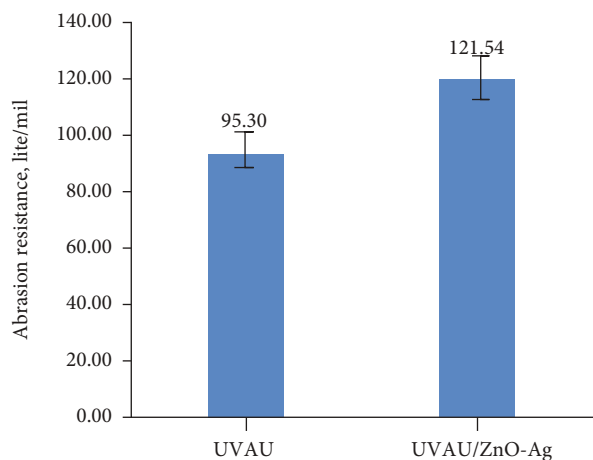


FIGURE 8: Abrasion resistance of the coating without (UVAU) and with 2 wt% ZnO-Ag nanohybrids (UVAU/ZnO-Ag) after 4.8 s of curing.

Figure 8 demonstrates that the incorporation of 2 wt% ZnO-Ag hybrid nanoparticles into polymer network helped gain the abrasion resistance of the paint film from 95.30 to 121.54 lites/mil. To explain the enhancement of abrasion

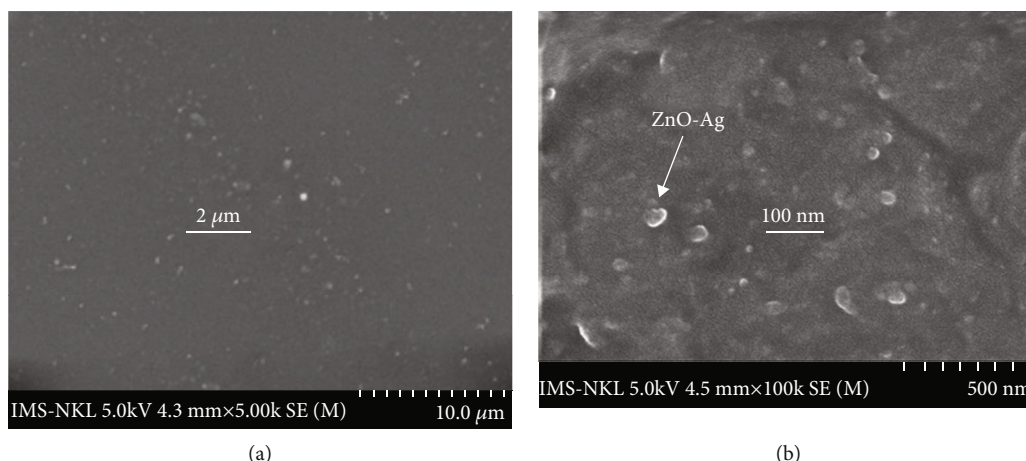


FIGURE 9: FE-SEM image of the photocurable acrylate urethane/ZnO-Ag nanocoating in surface (a) and in cross-section (b).

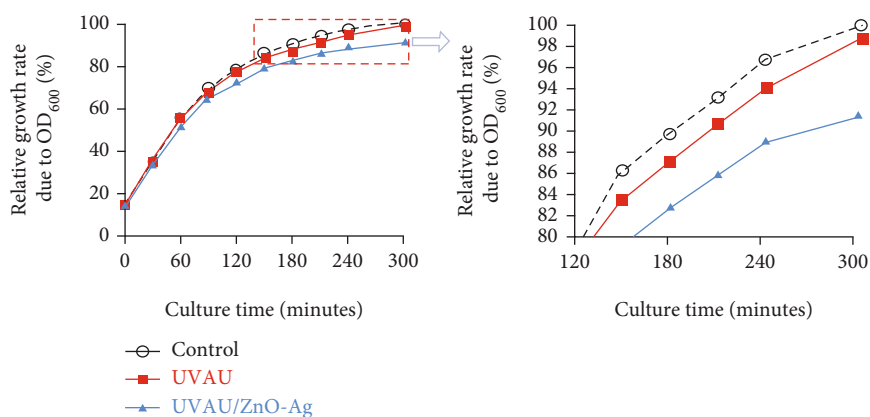


FIGURE 10: The growth rate of *E. coli* bacteria in liquid culture without (control) or with the presence of the coating films not containing (UVAU) or containing 2 wt% ZnO-Ag nanohybrids (UVAU/ZnO-Ag).

resistance of the photocurable acrylate urethane/ZnO-Ag nanocoating, its FE-SEM images are analyzed and indicated in Figure 9.

As can be seen from Figure 9, the coating possessed tight structures with no defects or cracks. Additionally, the nanohybrids are well-dispersed into the coating with a size of about 40-250 nm. The abrasion resistance of the nanocoating is enhanced by tough ZnO-Ag nanohybrids which had high hardness. This is also the reason for the increase in the relative hardness of the nanocoating in Figure 7.

3.3. Antimicrobial Activity of the Nanocoating. The growth rate of *E. coli* bacteria in liquid culture without (control) or with the presence of the coating films not containing (UVAU) or containing ZnO-Ag nanohybrids (UVAU/ZnO-Ag) during 300 min (5 h) is presented in Figure 10.

As shown in Figure 10, after 5 h of test, the growth rate of *E. coli* bacteria was only ~91% in the culture with added UVAU/ZnO-Ag coating (containing 2 wt% ZnO-Ag nanohybrids), whereas it was 98.5% in the culture with the presence of UVAU films (not containing 2 wt% ZnO-Ag nanohybrids). These results have proved that the UVAU/ZnO-Ag nanocomposite film has obviously stronger antibiotic effect against *E.*

coli bacteria than that of the UVAU/ZnO-Ag nanocomposite film [19].

4. Conclusion

ZnO-Ag nanohybrids were chemically synthesized in the aqueous medium by reducing silver nitrate with sodium borohydride NaBH_4 . Their structural morphology had been characterized by FE-SEM, TEM, and XRD. These nanohybrids (2 wt%) were then homogeneously dispersed into the diacrylate urethane/1,6-hexanediol diacrylate resin system. Photopolymerization, morphology and mechanical properties, and antimicrobial activity of UV curing acrylate urethane coating in the presence of 2 wt% ZnO-Ag nanohybrids were investigated. The analysis results show that ZnO-Ag nanohybrids are dispersed well in polymer matrix, with a size of about 40-250 nm. The nanohybrids enhance significantly both the conversion of acrylate groups, gel fraction, relative hardness, abrasion resistance, and antimicrobial activity of the coating. After 4.8 s crosslinking reaction, the conversion of acrylate groups, gel fraction, abrasion resistance, and hardness of the paint film increases from 93.53 to 95.82%, from 95.3 to 96.7%, from 0.72 to 0.76,

and from 95.28 to 121.54 l/mil, respectively. After 5 h of the antimicrobial test, the growth rate of *E. coli* bacteria is only ~91% in the culture with the presence of the paint films containing 2 wt% ZnO-Ag nanohybrids, while it is 98.5% in the culture with the presence of the films not containing the nanohybrids.

Data Availability

All the data and supporting materials are included within the article.

Conflicts of Interest

The authors declare no conflicts of interest.

Acknowledgments

The authors would like to thank the financial support of the Vietnam National Foundation for Science and Technology Development (NAFOSTED, Grant # 104.02-2018.19).

References

- [1] M. D. Brito, X. Allonas, C. Croutxé-Barghorn, M. Palmieri, and I. Alig, "Kinetic study of photoinduced quasi-simultaneous interpenetrating polymer networks," *Progress in Organic Coatings*, vol. 73, no. 2–3, pp. 186–193, 2012.
- [2] T. P. Nguyen-Tri and T. V. Nguyen, "Radically curable nano-based coatings (chapter 10)," in *Nanomaterials Based Coatings*, T. P. Nguyen, S. Rtimi, and C. Ouellet-Plamondon, Eds., pp. 339–372, Elsevier, 2019.
- [3] T. V. Nguyen, X. H. Le, P. H. Dao, C. Decker, and T. P. Nguyen, "Stability of acrylic polyurethane coatings under accelerated aging tests and natural outdoor exposure: the critical role of the used photo-stabilizers," *Progress in Organic Coatings*, vol. 124, pp. 137–146, 2018.
- [4] X. H. Le, T. V. Nguyen, M. T. Le, and T. V. T. Nguyen, "Study of photocrosslinking reaction of the resin system on the base of copolymer of tung and soybean oils, methyl methacrylate, styrene," *Vietnam Journal of Science Technology*, vol. 48, no. 3A, pp. 150–157, 2010.
- [5] C. M. Vu, L. T. Nguyen, T. V. Nguyen, and H. J. Choi, "Effect of additive-added epoxy on mechanical and dielectric characteristics of glass fiber reinforced epoxy composites," *Polymer Korea*, vol. 38, no. 6, pp. 726–734, 2014.
- [6] Q. V. Bach, C. M. Vu, H. T. Vu, T. Hoang, T. V. Dieu, and D. D. Nguyen, "Epoxidized soybean oil grafted with CTBN as a novel toughener for improving the fracture toughness and mechanical properties of epoxy resin," *Polymer Journal*, vol. 52, pp. 345–357, 2020.
- [7] C. M. Vu, V. H. Nguyen, and Q. V. Bach, "Phosphorous-jointed epoxidized soybean oil and rice husk-based silica as the novel additives for improvement mechanical and flame retardant of epoxy resin," *Journal of Fire Sciences*, vol. 38, no. 1, pp. 3–27, 2020.
- [8] Q. V. Bach, C. M. Vu, H. T. Vu, and D. D. Nguyen, "Enhancing mode I and II interlaminar fracture toughness of carbon fiber-filled epoxy-based composites using both rice husk silica and silk fibroin electrospun nanofibers," *High Performance Polymers*, vol. 31, no. 9–10, pp. 1195–1203, 2019.
- [9] D. D. Nguyen, C. M. Vu, and H. J. Choi, "Improvement of the mode I interlaminar fracture toughness of glass fiber/epoxy composites using polystyrene electrospun nanofibers," *Polymer Bulletin*, vol. 75, pp. 5089–5102, 2018.
- [10] C. M. Vu, Q. V. Bach, H. T. Vu, D. D. Nguyen, B. X. Kien, and S. W. Chang, "Carbon-fiber-reinforced epoxy resin with sustainable additives from silk and rice husks for improved mode-I and mode-II interlaminar fracture toughness," *Macromolecular Research*, vol. 28, no. 1, pp. 33–41, 2020.
- [11] C. M. Vu and H. J. Choi, "Fracture toughness and surface morphology of micro/nano sized fibrils-modified epoxy resin," *Polymer Science Series A*, vol. 58, no. 3, pp. 464–470, 2016.
- [12] C. M. Vu and Q. V. Bach, "Effects of DOPO-grafted epoxidized soybean oil on fracture toughness and flame retardant of epoxy resin/rice husk silica hybrid," *Macromolecular Research*, vol. 28, no. 9, pp. 826–834, 2020.
- [13] T. V. Nguyen, T. A. Nguyen, P. H. Dao et al., "Effect of rutile titania dioxide nanoparticles on the mechanical property, thermal stability, weathering resistance and antibacterial property of styrene acrylic polyurethane coating," *Advances in Natural Sciences: Nanoscience and Nanotechnology*, vol. 7, no. 4, 2016.
- [14] A. M. El Saeed, M. A. El-Fattah, and A. M. Azzam, "Synthesis of ZnO nanoparticles and studying its influence on the antimicrobial, anticorrosion and mechanical behavior of polyurethane composite for surface coating," *Dyes and Pigments*, vol. 121, pp. 282–289, 2015.
- [15] H. Barani, "Preparation of antibacterial coating based on in situ synthesis of ZnO/SiO₂ hybrid nanocomposite on cotton fabric," *Applied Surface Science*, vol. 320, pp. 429–434, 2014.
- [16] P. Dallas, V. K. Sharma, and R. Zboril, "Silver polymeric nanocomposites as advanced antimicrobial agents: classification, synthetic paths, applications, and perspectives," *Advances in Colloid and Interface Science*, vol. 166, no. 1–2, pp. 119–135, 2011.
- [17] M. Akbarian, M. E. Olya, M. Ataefard, and M. Mahdavian, "The influence of nanosilver on thermal and antibacterial properties of a 2 K waterborne polyurethane coating," *Progress in Organic Coatings*, vol. 75, no. 4, pp. 344–348, 2012.
- [18] R. D. Toker, N. Kayaman-Apohan, and M. V. Kahraman, "UV-curable nano-silver containing polyurethane based organic-inorganic hybrid coatings," *Progress in Organic Coatings*, vol. 76, no. 9, pp. 1243–1250, 2013.
- [19] T. T. Le, T. V. Nguyen, T. A. Nguyen et al., "Thermal, mechanical and antibacterial properties of water-based acrylic polymer/SiO₂-Ag nanocomposite coating," *Journal of Materials Chemistry and Physics*, vol. 232, pp. 362–366, 2019.
- [20] T. P. Nguyen, T. A. Nguyen, T. H. Nguyen, and P. Carriere, "Antibacterial behavior of hybrid nanoparticles (Chapter 7)," in *Noble Metal-Metal Oxide Hybrid Nanoparticles: Fundamentals and Applications*, S. Mohapatra, T. A. Nguyen, and T. P. Nguyen, Eds., pp. 141–155, Woodhead Publishing, 2019.
- [21] T. D. Ngo, T. M. H. Le, T. H. Nguyen et al., "Antibacterial nanocomposites based on Fe₃O₄-Ag hybrid nanoparticles and natural rubber-polyethylene blends," *International Journal of Polymer Science*, vol. 2016, Article ID 7478161, 9 pages, 2016.
- [22] T. N. L. Nguyen, T. V. Do, T. V. Nguyen et al., "Antimicrobial activity of acrylic polyurethane/Fe₃O₄-Ag nanocomposite coating," *Progress in Organic Coatings*, vol. 132, pp. 15–20, 2019.
- [23] T. V. Nguyen, T. V. Do, M. H. Ha et al., "Crosslinking process, mechanical and antibacterial properties of UV-curable acrylate/Fe₃O₄-Ag nanocomposite coating," *Journal of Progress in organic coating*, vol. 139, p. 105325, 2020.

- [24] N. Huong, "Improvement of bearing strength of laminated composites by nanoclay and Z-pin reinforcement," *PhD. Dissertation*, University of New South Wales, Australia, 2006.
- [25] O. Becker, R. Varley, and G. Simon, "Morphology, thermal relaxations and mechanical properties of layered silicate nanocomposites based upon high-functionality epoxy resins," *Polymer*, vol. 43, no. 16, pp. 4365–4373, 2002.
- [26] M. Jouyandeh, M. Shabaniyan, M. Khaleghi et al., "Acid-aided epoxy-amine curing reaction as reflected in epoxy/Fe₃O₄ nanocomposites: chemistry, mechanism, and fracture behavior," *Progress in Organic Coatings*, vol. 125, pp. 384–392, 2018.
- [27] M. Jouyandeh, S. M. R. Paran, M. Shabaniyan et al., "Curing behavior of epoxy/Fe₃O₄ nanocomposites: a comparison between the effects of bare Fe₃O₄, Fe₃O₄/SiO₂/chitosan and Fe₃O₄/SiO₂/chitosan/imide/phenylalanine-modified nanofillers," *Progress in Organic Coatings*, vol. 123, pp. 10–19, 2018.
- [28] M. R. Saeb, M. Nonahal, H. Rastin et al., "Calorimetric analysis and molecular dynamics simulation of cure kinetics of epoxy/chitosan-modified Fe₃O₄ nanocomposites," *Progress in Organic Coatings*, vol. 112, pp. 176–186, 2017.
- [29] M. R. Saeb, H. Rastin, M. Shabaniyan, M. Ghaffari, and G. Bahlakeh, "Cure kinetics of epoxy/ β -cyclodextrin-functionalized Fe₃O₄ nanocomposites: Experimental analysis, mathematical modeling, and molecular dynamics simulation," *Progress in Organic Coatings*, vol. 110, pp. 172–181, 2017.
- [30] H. Yari, S. Moradian, and N. Tahmasebi, "The weathering performance of acrylic melamine automotive clearcoats containing hydrophobic nanosilica," *Journal Coating Technology and Research*, vol. 11, no. 3, pp. 351–360, 2014.
- [31] T. M. A. Bui, T. V. Nguyen, T. M. Nguyen et al., "Investigation of crosslinking, mechanical properties and weathering stability of acrylic polyurethane coating reinforced by SiO₂ nanoparticles issued from rice husk ash," *Journal of Materials Chemistry and Physics*, vol. 241, p. 122445, 2020.
- [32] P. H. Dao, T. V. Nguyen, M. H. Dang et al., "Effect of silica nanoparticles on properties of coatings based on acrylic emulsion resin," *Vietnam Journal of Science and Technology*, vol. 56, no. 3B, pp. 117–125, 2018.
- [33] T. V. Nguyen, T. A. Nguyen, and T. H. Nguyen, "The synergistic effects of SiO₂ nanoparticles and organic photostabilizers for enhanced weathering resistance of acrylic polyurethane coating," *Journal of Composites Science*, vol. 4, no. 1, p. 23, 2020.
- [34] T. V. Nguyen, T. P. Nguyen, S. Azizi et al., "The role of organic and inorganic UV-absorbents on photopolymerization and mechanical properties of acrylate-urethane coating," *Journal of Materials Today Communications*, vol. 22, p. 100780, 2020.
- [35] T. V. Nguyen, P. H. Dao, T. A. Nguyen et al., "Photocatalytic degradation and heat reflectance recovery of water-borne acrylic polymer/ZnO nanocomposite coating," *Journal of Applied Polymer Science*, vol. 137, no. 37, p. 49116, 2020.
- [36] P. H. Dao, T. V. Nguyen, T. A. Nguyen et al., "Acrylic polymer/TiO₂ nanocomposite coatings: mechanism for photo-degradation and solar heat reflective recovery," *Journal of Materials Chemistry and Physics*, vol. 272, p. 124984, 2021.
- [37] T. V. Vu, T. V. Nguyen, M. Tabish et al., "Water-borne ZnO/acrylic nanocoating: fabrication, characterization, and properties," *Polymers*, vol. 13, no. 5, p. 717, 2021.
- [38] T. V. Nguyen, T. P. Nguyen, T. D. Nguyen, R. Aidani, V. T. Trinh, and C. Decker, "Accelerated degradation of water borne acrylic nanocomposites used outdoor protective coatings," *Polymer Degradation and Stability*, vol. 128, pp. 65–76, 2016.
- [39] T. V. Nguyen, P. H. Dao, K. L. Duong et al., "Effect of R-TiO₂ and ZnO nanoparticles on the UV-shielding efficiency of water-borne acrylic coating," *Progress in Organic Coatings*, vol. 110, pp. 114–121, 2017.
- [40] T. A. T. Pham, V. A. Tran, V. D. Le et al., "Facile preparation of ZnO nanoparticles and Ag/ZnO nanocomposite and their photocatalytic activities under visible light," *International Journal of Photoenergy*, vol. 2020, Article ID 8897667, 2020.